

Pericardium Based Model Fusion of CT and Non-contrasted C-arm CT for Visual Guidance in Cardiac Interventions

Yefeng Zheng

Imaging and Computer Vision, Siemens Corporation, Corporate Technology,
Princeton, NJ, USA

yefeng.zheng@siemens.com

Abstract. Minimally invasive transcatheter cardiac interventions are being adopted rapidly to treat a range of cardiovascular diseases. Pre-operative imaging, *e.g.*, computed tomography (CT), plays an important role in surgical planning and simulation of cardiac interventions. Overlaying a 3D cardiac model extracted from pre-operative images onto real-time fluoroscopic images provides valuable visual guidance during the intervention. However, direct 3D to 2D fusion is difficult and may require quite amounts of user interaction. Intra-operative non-contrasted C-arm CT can be used as an intermedium for model fusion. The cardiac model is first warped to C-arm CT and later overlaid onto fluoroscopy. The C-arm CT to fluoroscopy overlay is straightforward since both images are captured on the same machine and the C-arm projection geometry can be directly used for overlay. Though various image registration methods may be used to fuse pre-operative images and C-arm CT, cross-modality image registration is not robust due to the significant difference in image characteristics (contrasted vs. non-contrasted). In this work we propose a model based fusion method using the pericardium to align pre-operative CT to intra-operative C-arm CT. After automatic segmentation of the pericardium in both CT and C-arm CT, the deformation field is estimated and then applied to warp the cardiac model extracted from CT to C-arm CT. The proposed method can be applied to fuse different cardiac models (*e.g.*, chambers, aorta, coronary arteries, and cardiac valves). A feasibility study on aortic root model fusion shows that a reasonable accuracy can be achieved using a generic model (from a different patient), while more accurate results come from a patient-specific model. Intelligently weighted fusion can further improve the accuracy by using all available cardiac models in a pre-collected training set.

1 Introduction

Minimally invasive transcatheter cardiac interventions are being adopted rapidly, especially for high-risk patients, to treat a wide range of cardiovascular diseases, including endovascular stenting of coronary stenoses, transcatheter aortic valve implantation (TAVI) [1], and cardiac arrhythmia ablation, etc. Pre-operative imaging from various modalities, *e.g.*, computed tomography (CT), magnetic resonance imaging (MRI), and

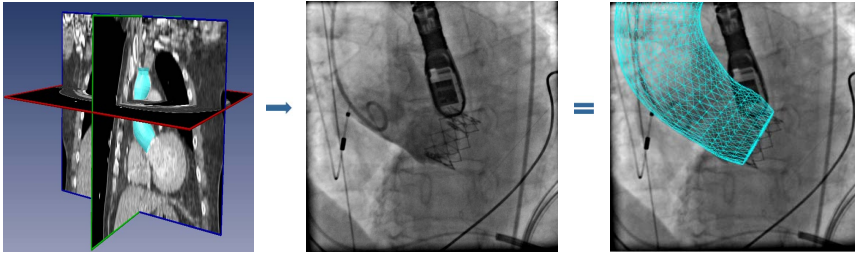


Fig. 1. Direct 3D to 2D fusion of the aortic root model to provide visual guidance for transcatheter aortic valve implantation. **Left:** Pre-operative 3D CT with the automatically segmented aortic root mesh. **Middle:** A 2D fluoroscopic image with contrast injection inside the aortic root. **Right:** Model fusion result. Direct 3D to 2D fusion is difficult and manual interaction may be required.

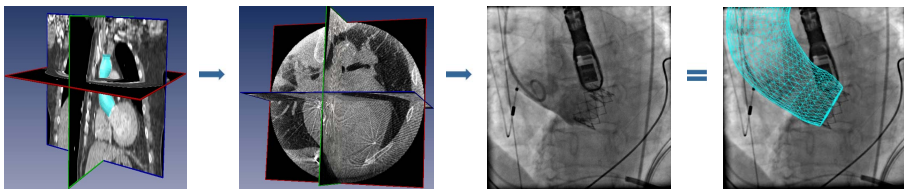


Fig. 2. Non-contrasted C-arm CT based fusion of the aortic root model to provide visual guidance for transcatheter aortic valve implantation. **Left:** Pre-operative 3D CT with the automatically segmented aortic root mesh. **Left Middle:** Intra-operative non-contrasted C-arm CT. **Right Middle:** A 2D fluoroscopic image. **Right:** Model fusion result.

ultrasound, are often scanned for planning, simulation, and intra-operative visual guidance of the intervention [2]. These images often provide detailed delineation of cardiac structures (*e.g.*, in CT/MRI) or cardiac motion information (*e.g.*, cine MRI and real-time ultrasound). Overlaying the cardiac model extracted from pre-operative images onto real-time fluoroscopic images provides valuable visual guidance during the surgery. However, direct fusion of the 3D model with an intra-operative fluoroscopic image (often called 3D-to-2D registration) is difficult because the images are captured at different times, on different scanning machines, and sometimes from different cardiac phases. Fig. 1 shows the workflow of direct 3D to 2D fusion of the aortic root model. This procedure normally needs some amount of user interaction and contrast agent injection is often required to highlight the target anatomy (the aortic root in this case) to facilitate the registration [3]. However, due to the side effects (*e.g.*, renal failure), the use of contrast agent should be minimized and, ideally, completely avoided.

Recently, intra-operative C-arm CT is emerging as a new imaging modality for cardiac interventions. C-arm CT is created by rotating the C-arm X-ray source/detector around the patient during the intervention. The imaging is performed intra-operatively, therefore it manifests patient anatomy at the time of the operation. Since the 3D C-arm CT and 2D fluoroscopic images are captured on the same machine (a C-arm system), the 3D-to-2D registration is straightforward using the projection geometry. However, performing a high-quality motion compensated/contrasted C-arm CT scan is not feasible

for most patients due to the slow gantry rotation speed of C-arm. Intravenous or trans-catheter injection of contrast agent requires extra preparation and wiring in a crowded hybrid operating room. It is much easier to scan a non-ECG-gated and non-contrasted intra-operative C-arm CT. Though the target anatomy may be hardly visible and difficult to segment, non-contrasted C-arm CT can act as an intermedium to bring the 3D cardiac model extracted from pre-operative images to fluoroscopic images. Fig. 2 shows the fusion of pre-operative CT to fluoroscopy using non-contrasted C-arm CT as an intermedium. The fusion of CT to C-arm CT is easier than the direct fusion from 3D CT to 2D fluoroscopy and contrast injection in fluoroscopy is not necessary. An additional C-arm CT scan will incur more radiation. However, since patients undergoing cardiac interventions are normally in their advanced ages, if there is cancer caused by radiation, it will probably occur much later than the expected life span of the patients. Contrast-induced nephropathy is an acute complication and is very common in such patient population. Therefore, radiation is less a concern than contrast-induced nephropathy.

Image registration may be used to estimate the deformation field from pre-operative images to C-arm CT for model fusion [4]. Due to the significant difference in image characteristics (contrasted vs. non-contrasted), cross-modality image registration is difficult. If the transformation between pre- and intra-operative images is large, the registration is likely to fail. Furthermore, image registration is very time consuming, especially for non-rigid registration.

In this work we propose a model based fusion method to align pre-operative images and C-arm CT. First, we need to identify an anchor structure that is present in both pre-operative images and C-arm CT. The anchor structure also needs to be easy to be segmented reliably. Using the segmented anchor structure, we can then estimate the deformation field and use it to warp the cardiac model to C-arm CT. For the particular application on the fusion of pre-operative CT and C-arm CT for cardiac interventions, we find that the pericardium (the outer surface of the heart) is a reliable anchor structure. It is clearly visible in both CT and C-arm CT. A robust segmentation system can be developed for both contrasted and non-contrasted data. After pericardium segmentation, the thin-plate-spline model [5] is used to estimate the deformation field. Due to the proximity to the pericardium, the deformation of cardiac structures (*e.g.*, chambers, aorta, and valves) can be inferred well from the deformation of the pericardium. The proposed method is computationally much more efficient than the image registration based approach. It is also fully automatic. A feasibility study on aortic root model fusion shows that a reasonable accuracy can be achieved using a generic model (from a different patient), while more accurate results come from a patient-specific model. Intelligently weighted fusion can further improve the accuracy by using all available cardiac models in a pre-collected training set.

2 Pericardium Based Model Fusion

2.1 Automatic Pericardium Segmentation

Various pericardium segmentation methods have been proposed in the literature, *e.g.*, the atlas based methods [6,7], graph cuts [8], or constrained segmentation by the

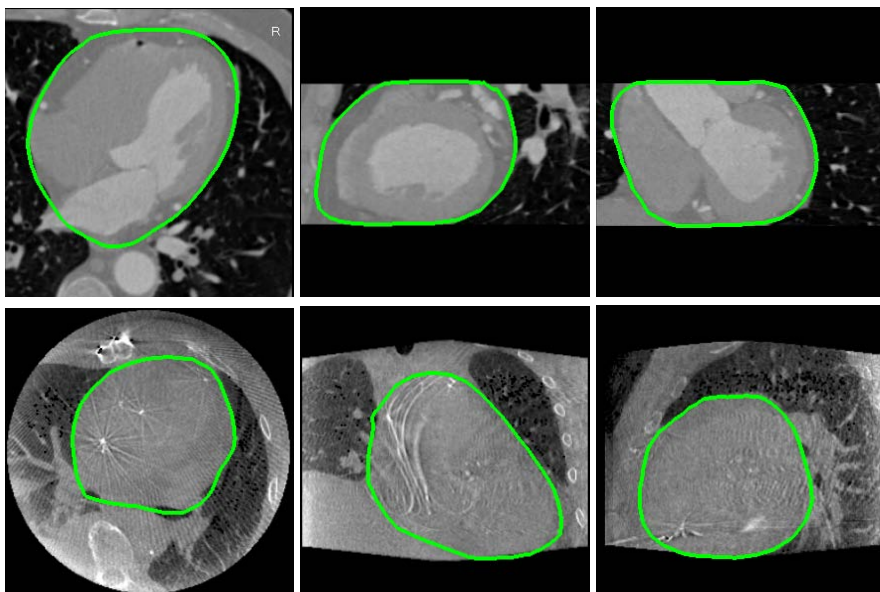


Fig. 3. Pericardium segmentation on a contrasted CT scan (top row) and a non-contrasted C-arm CT scan (bottom row). From left to right three orthogonal cuts of the volume are shown.

neighboring lungs [9,10]. All these methods are pretty time consuming, taking at least 20 seconds [8] and may be up to 30 minutes [6]. They often only work on one kind of images, either contrasted or non-contrasted, but not both as required in this application.

In this work we adapt the marginal space learning (MSL) method [11,12] for efficient and fully automatic segmentation of the pericardium. First, MSL is exploited to estimate the position, orientation, and size of the heart. A mean shape (which is trained on a set of example shapes) is then aligned with the estimated pose as an initial estimate of the pericardium boundary. We then use learning based boundary detectors to guide the boundary evolution under the active shape model (ASM) framework. Our approach is more robust than the previous methods and works on both contrasted and non-contrasted scans. It runs at about 1.5 s/volume, which is at least 10 times faster than the previous methods [6,7,8]. Using a model-based approach, the segmented pericardium mesh points have built-in anatomical correspondence across volumes, which facilitates the deformation field estimation afterward. Fig. 3 shows pericardium segmentation results on contrasted CT and non-contrasted C-arm CT.

2.2 Deformation Field Estimation

The segmented pericardium meshes from both imaging modalities are used to estimate the deformation field for model fusion. We use the well-known thin-plate-spline (TPS) model to estimate the deformation field $f(x, y, z)$, which minimizes the bending energy E of a thin plate,

$$E = \int_{\mathcal{R}^3} \left(\frac{\partial^2 f}{\partial x^2} \right)^2 + \left(\frac{\partial^2 f}{\partial y^2} \right)^2 + \left(\frac{\partial^2 f}{\partial z^2} \right)^2 + 2 \left(\frac{\partial^2 f}{\partial x \partial y} \right)^2 + 2 \left(\frac{\partial^2 f}{\partial x \partial z} \right)^2 + 2 \left(\frac{\partial^2 f}{\partial y \partial z} \right)^2 dx dy dz \quad (1)$$

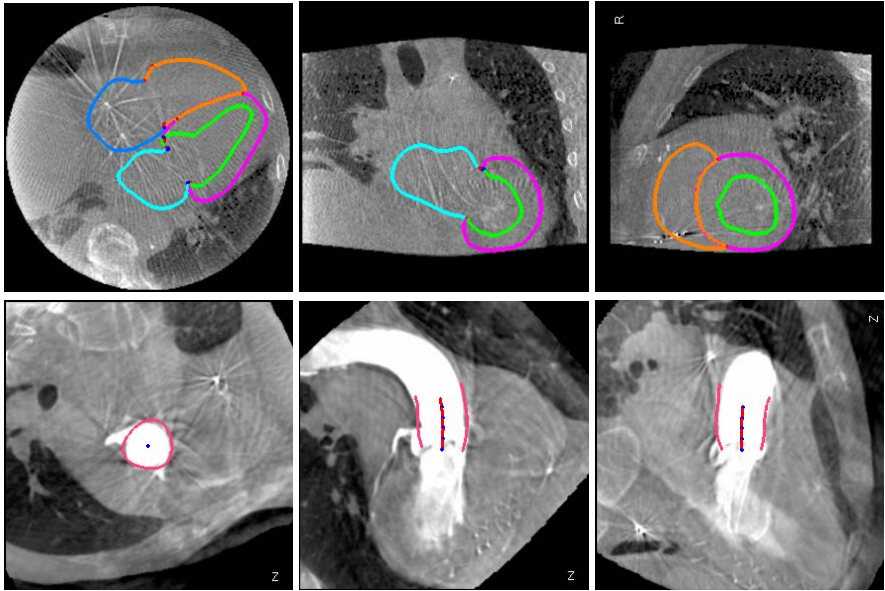


Fig. 4. Warping of cardiac models extracted from CT to C-arm CT using segmented pericardium from both imaging modalities. Top row shows the warped four-chamber heart model on non-contrasted C-arm CT and the bottom row shows the warped aortic root model on contrasted C-arm CT. From left to right three orthogonal cuts of the volume are shown.

Other parametric or non-parametric deformation fields can also be used. We choose the TPS deformation model because (1) the interpolation is smooth with derivatives of any order; (2) the model has no free parameters that need manual tuning; (3) it has closed-form solutions for both warping and parameter estimation; and (4) there is a physical explanation for its energy function. Details of the TPS model can be found in [5].

The cardiac models extracted from CT is then transferred to C-arm CT using the estimated deformation field. The top row of Fig. 4 shows a warped four-chamber heart model [11] in non-contrasted C-arm CT. The cardiac chambers are configured properly at a roughly correct position, although it is difficult to check the precision of the fused model due to the lack of contrast inside the heart. An example of the warped aortic root model on contrasted C-arm CT is also shown in the bottom row of Fig. 4, which clearly shows the accuracy of the warping.

2.3 Intelligently Weighted Average for Model Fusion

A feasibility study of model fusion for the aortic root (refer to Section 3) shows that the prediction using a patient-specific model is more accurate than a generic model (4.18 *mm* vs. 5.00 *mm*). However, even with a patient-specific model, the prediction still has room for improvement since the CT and C-arm CT are scanned at different times, from different cardiac phases, and with complicated non-rigid deformation between scans. It is a waste of resource to solely use the pre-operative data from the same patient for

model fusion. In this work we propose an intelligently weighted average method to make full use of the pre-operative models from both the same and different patients.

Suppose we already have n patients in our heart model library. For each patient the target heart model m_1, m_2, \dots, m_n (e.g., chambers or aorta) and the pericardium p_1, p_2, \dots, p_n are already segmented and manual corrected if necessary. Given an input patient with both CT and C-arm CT data available, we first perform segmentation to get the target heart model m_0 and pericardium p_0 from CT. We also segment the pericardium q from C-arm CT. For each patient i for $i = 0, 1, \dots, n$, using the segmented pericardium meshes from both pre-operative and intra-operative images, we can predict the target model a_i in C-arm CT. The final prediction is a weighted average of the aligned models (surface meshes) a_0, a_1, \dots, a_n . The question is how to set the weights properly to generate an accurate fused model a . In this work the weight is set according to the shape distance between pericardium meshes p_i and q . The underlying philosophy is that if two patients have a similar shape in the pericardium, they are likely to have a similar shape in the target cardiac structure. This assumption is reasonable and intuitive since the pericardium encloses all cardiac anatomies and is only a few millimeters away from the free-wall epicardium of all four chambers. The shape of the pericardium is highly correlated to the inner cardiac anatomies. Therefore, if the pericardium shape distance $d(p_i, q)$ is small, we should assign a large weight to the predicted model a_i . The pericardium shape distance $d(p_i, q)$ is defined as the average point-to-point distance between two meshes after compensating the similarity transformation. The distance is further converted to a weight

$$w_i = 1 - \frac{d_i - d_{min}}{d_{max} - d_{min}}, \quad (2)$$

where d_{min} and d_{max} is the minimum and maximum value of $\{d_0, d_1, \dots, d_n\}$, respectively. It is easy to verify that the patient with the most similar pericardium shape has a weight of one and the patient with the most dissimilar shape has a weight of zero. There are many ways to calculate the final weighted fusion. In this work we use a simple weighted average

$$a = \frac{\sum_{i=0}^n w_i a_i}{\sum_{i=0}^n w_i}. \quad (3)$$

Since the target models a_i are segmented using a model-based approach with built-in correspondence, the weighted average is simple arithmetic average of the mesh point positions.

3 Experiments

In this section we evaluate the model fusion accuracy for the aortic root in the TAVI application. Sixteen CT and C-arm CT pairs were collected from a clinical site. The CT data was captured from various cardiac phases for different patients. The C-arm CT was scanned under rapid ventricular pacing and direct contrast injection inside the aortic root. Although the target application is to use non-ECG-gated non-contrasted C-arm CT, it is impossible to quantitatively evaluate the model fusion accuracy on such

Table 1. Quantitative evaluation of the model fusion accuracy for the aortic root from pre-operative CT to intra-operative C-arm CT on 16 datasets. The mesh-to-mesh distance is reported in millimeters.

	Mean	Std	Median	80 th Percentile
Same Patient (Affine)	5.60	1.91	5.76	6.18
Same Patient (TPS)	4.18	1.47	4.29	5.42
Different Patient (TPS)	5.00	1.92	4.59	5.13
Intelligently Weighted Fusion	3.62	1.44	3.66	4.39

data. On the TAVI data, the aortic root is clearly visible from both CT and C-arm CT, which makes possible for a quantitative evaluation. Due to the difference in scanning protocol, the reported registration accuracy in this experiment may be more optimistic than the real application scenario.

The aortic root is segmented in both CT and C-arm CT using a method presented in [1], resulting in almost perfect segmentation. The segmented aortic root in CT is not corrected, however, little manual correction is performed to generate the ground-truth aortic root mesh in C-arm CT for the following quantitative evaluation. The pericardium is also automatically segmented in both CT and C-arm CT using the method described in Section 2.1. The pericardium segmentation is excellent with only minor errors on some data. However, these errors are not corrected to mimic the real clinical application. The aortic root model extracted from CT is then aligned to C-arm CT using the segmented pericardium (with one example shown in the bottom row of Fig. 4). We then calculate the quantitative mesh-to-mesh distance from the predicted aortic root boundary to the true boundary in C-arm CT.

We first compare the accuracy using the affine transformation and the TPS transformation for model fusion using the patient-specific model. As shown in Table 1, the mean mesh error is about 5.60 *mm* under the affine transformation, compared to 4.18 *mm* under the TPS transformation. It is clear that the non-rigid TPS transformation can achieve more accurate result. It is also more accurate using a patient-specific model. If the aortic root model from a different patient is used, the mean mesh prediction error increases to 5.00 *mm*. However, if the predicted models from all patients are fused with proper weights according to Eq. (1), we can achieve the best result with a mean error of 3.62 *mm*.

4 Conclusions

In this work we proposed to use the pericardium to align pre-operative CT to intra-operative C-arm CT for model fusion with applications to transcatheter cardiac interventions. Visually accurate prediction of the aortic root and four heart chambers can be achieved on non-contrasted C-arm CT. A quantitative evaluation on contrasted C-arm CT data shows that a small mean error (3.62 *mm*) can be achieved for the aortic root prediction. Using a patient-specific model achieves more accurate prediction than using models from different patients. Intelligently weighted fusion using all available models can further reduce the prediction error. Using C-arm CT as an intermedium, the aligned pre-operative CT can be projected to real-time fluoroscopy images using the C-arm coordinate system. The most important application of the overlaid model is to provide

3D orientation information of the target anatomy. It also helps a physician (especially a junior one) in rough positioning of the interventional devices. According to the feedback from our collaborating physicians, a mean error of 3.62 mm is sufficient for such clinical applications. Even though one contrast injection is still necessary to confirm the device position before final deployment, the proposed method can reduce the number of contrast injections (ideally to just one before the final deployment).

In the future we will investigate the accuracy of the aligned 3D model projected onto 2D fluoroscopy images. The proposed method provides an automatic alignment with pretty reasonable accuracy. Minor local adjustment can further compensate the cardiac motion and respiratory motion observed in real-time cardiac fluoroscopy [3].

References

1. Zheng, Y., John, M., Liao, R., Nottling, A., Boese, J., Kempfert, J., Walther, T., Brockmann, G., Comaniciu, D.: Automatic aorta segmentation and valve landmark detection in C-arm CT for transcatheter aortic valve implantation. *IEEE Trans. Medical Imaging* 31(12), 2307–2321 (2012)
2. Schoenhagen, P., Numburi, U., Halliburton, S.S., et al.: Three-dimensional imaging in the context of minimally invasive and transcatheter cardiovascular interventions using multi-detector computed tomography: From pre-operative planning to intra-operative guidance. *European Heart Journal* 31(22), 2727–2740 (2010)
3. Miao, S., Liao, R., Zheng, Y.: A hybrid method for 2-D/3-D registration between 3-D volumes and 2-D angiography for trans-catheter aortic valve implantation (TAVI). In: *Proc. IEEE Int'l Sym. Biomedical Imaging*, pp. 1215–1218 (2011)
4. Maintz, J., Viergever, M.: A survey of medical image registration. *Medical Image Analysis* 2(1), 1–36 (1998)
5. Bookstein, F.: Principal warps: Thin-plate splines and the decomposition of deformations. *IEEE Trans. Pattern Anal. Machine Intell.* 11(6), 567–585 (1989)
6. van Rikxoort, E.M., Isgum, I., Staring, M., Klein, S., van Ginneken, B.: Adaptive local multi-atlas segmentation: Application to heart segmentation in chest CT scans. In: *Proc. of SPIE Medical Imaging* (2008)
7. Lelieveldt, B.P.F., van der Geest, R.J., Rezaee, M.R., Bosch, J.G., Reiber, J.H.C.: Anatomical model matching with fuzzy implicit surfaces for segmentation of thoracic volume scans. *IEEE Trans. Medical Imaging* 18(3), 218–230 (1999)
8. Funka-Lea, G., Boykov, Y., Florin, C., Jolly, M.P., Moreau-Gobard, R., Ramaraj, R., Rinck, D.: Automatic heart isolation for CT coronary visualization using graph-cuts. In: *Proc. IEEE Int'l Sym. Biomedical Imaging*, pp. 614–617 (2006)
9. Gregson, P.H.: Automatic segmentation of the heart in 3D MR images. In: *Canadian Conf. Electrical and Computer Engineering*, pp. 584–587 (1994)
10. Moreno, A., Takemura, C.M., Colliot, O., Camara, O., Bloch, I.: Using anatomical knowledge expressed as fuzzy constraints to segment the heart in CT images. *Pattern Recognition* 41(8), 2525–2540 (2008)
11. Zheng, Y., Barbu, A., Georgescu, B., Scheuering, M., Comaniciu, D.: Four-chamber heart modeling and automatic segmentation for 3D cardiac CT volumes using marginal space learning and steerable features. *IEEE Trans. Medical Imaging* 27(11), 1668–1681 (2008)
12. Zheng, Y., Vega-Higuera, F., Zhou, S.K., Comaniciu, D.: Fast and automatic heart isolation in 3D CT volumes: Optimal shape initialization. In: *Int'l Workshop on Machine Learning in Medical Imaging (In conjunction with MICCAI)* (2010)